

---

## Inhibitory effect of some benzothiazole derivatives on corrosion of mild steel: A computational study

M. Dehdab, M. Shahraki and S. M. Habibi-Khorassani\*

*Department of Chemistry, Faculty of Science, University of Sistan and Baluchestan,  
P. O. Box 98135-674, Zahedan, Iran*

*E-mails: [smhabibi@chem.usb.ac.ir](mailto:smhabibi@chem.usb.ac.ir) & [smhabibius@yahoo.com](mailto:smhabibius@yahoo.com)*

---

### Abstract

Inhibitory Effect of three benzothiazole derivatives (1, 3-benzothiazol-2-amine (BTA), 6-methyl-1, 3-benzothiazol-2-amine (MBTA) and 2-amino-1, 3-benzothiazole-6-thiol (TBTA)) on corrosion of carbon steel has been studied using density functional theory (DFT) method in gas and aqueous phases. Quantum chemical parameters such as  $E_{\text{HOMO}}$  (highest occupied molecular orbital energy),  $E_{\text{LUMO}}$  (lowest unoccupied molecular orbital energy), hardness ( $\eta$ ), polarizability ( $\alpha$ ), surface area and total negative charges on atoms (TNC) have been calculated at the B3LYP level of theory with 6-311++G\*\* basis set. The Mulliken charges of the molecules were also computed and Atoms-in-Molecule (AIM) method suggested the Fe-inhibitor interactions in these compounds are partially covalent and partially electrostatic. In good agreement with the experimental data, theoretical results showed the order of inhibitory efficiency is TBTA > MBTA > BTA.

**Keywords:** Corrosion; inhibitor; Benzothiazol; DFT; AIM

---

### 1. Introduction

Evaluation of corrosion inhibitors for mild steel in acidic media is important from both theoretical and industrial points of views (Ergun, Yüzer, & Emregül, 2008; Umoren & Obot, 2008). Compounds containing hetero atoms in their aromatic or long carbon chain are capable of being adsorbed on the metal surface and can protect the metal against corrosion. For this class of compounds, the presence of hetero atoms (nitrogen, sulphur, oxygen and even selenium and phosphorous) and  $\pi$ -electrons in their double or triple bonds have been found to help the adsorption of the metal (Gopi, Govindaraju, & Kavitha, 2010; Sethuraman & Raja, 2005). Benzothiazoles have been used as corrosion inhibitors for steel (Al-Mayout, Al-Suhybani, & Al-Ameery, 1998; Quraishi, Ansari, Ahmad, & Venkatachari, 1998; Quraishi, Wajid Khan, Ajmal, Muralidharan, & Venkatakrishna Iyer, 1996) copper (Zhou, Feng, Wu, Notoya, & Ishikawa, 1993) and brass (Nataraja, Venkatesha, & Tandon, 2012). Benzothiazole has two heteroatoms N and S in the thiazole ring. These heteroatoms have the ability to coordinate with transition metals through the d-orbitals of the metals and empty p- or d-orbitals of heteroatoms in the inhibitor molecules. In addition, the  $\pi$  orbitals of the benzene ring can overlap with the metal d-orbitals leading to bond formation.

Recently, DFT methods have been used to analyze the characteristics of the inhibitor/surface mechanism and to describe the structural nature of the inhibitor in the corrosion process (Rodríguez-Valdez, Martínez-Villafañe, & Glossman-Mitnik, 2005; D. Wang et al., 1999). Recently, Patel et al. (2014) have experimentally reported inhibitory efficiencies of benzothiazole derivatives as 1,3-benzothiazol-2-amine (BTA), 6-methyl-1,3-benzothiazol-2-amine (MBTA) and 2-amino-1,3-benzothiazole-6-thiol (TBTA) against mild steel corrosion in 1 N HCl solutions.

In the present work, we investigated theoretically the inhibitory efficiency of three benzothiazole derivatives (1, 3-benzothiazol-2-amine (BTA), 6-methyl-1, 3-benzothiazol-2-amine (MBTA) and 2-amino-1, 3-benzothiazole-6-thiol (TBTA)) using DFT and AIM methods (Fig. 1). Some quantum chemical parameters such as  $E_{\text{HOMO}}$  (highest occupied molecular orbital energy),  $E_{\text{LUMO}}$  (lowest unoccupied molecular orbital energy), hardness ( $\eta$ ), polarizability ( $\alpha$ ), Surface area and total negative charges on atoms (TNC) were evaluated and the results compared with experimental data. This work displays a good correlation between the theoretical and experimental data which confirms the reliability of the quantum chemical methods for studying inhibiting corrosion of metal surfaces.

---

\*Corresponding author

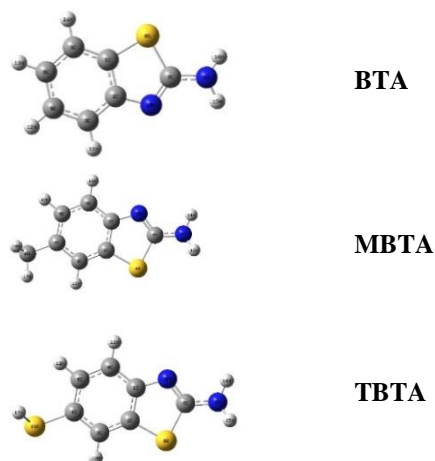


**Fig. 1.** Optimized structures for three benzothiazole derivatives (1, 3-benzothiazol-2-amine (BTA), 6-methyl-1, 3-benzothiazol-2-amine (MBTA) and 2-amino-1, 3-benzothiazole-6-thiol (TBTA))

## 2. Computational methods

Quantum chemical calculations were performed for benzothiazol derivatives as corrosion inhibitors using the density functional theory (DFT) method at the hybrid functional B3LYP level of theory with 6-311++G\*\* basis set (Becke, 1988; Becke, 1993; Lee, Yang, & Parr, 1988) by the Gaussian 03 series of programs (Frisch, 2004). Frequency calculations were also carried out on optimized geometries to find out the nature of the stationary point on the potential energy surface.

The theoretical parameters were calculated in gas phase while the electrochemical corrosion phenomena occur in an aqueous phase. For this reason, the polarizable continuum method (PCM) was employed to incorporate the solvent effect (water) in the calculations. The computational study was first carried out in the gas phase, then the self-consistent reaction field (SCRF) theory (Becke, 1988), with Tomasi's polarized continuum model (PCM) was used to better approach the experimental results obtained from the aqueous solution (Yang & Mortier, 1986). Indeed, this method models the solvent as a continuum of uniform dielectric constant and defines the cavity where the solute is placed as a uniform series of interlocking atomic spheres. Since the theoretical calculation cannot represent the effect of hydrogen chloride solution, water was used instead to include the solvent effect. In the acidic environment the inhibitors also interact with the acidic solution leading to the possibility of co-existence between both the protonated and non-protonated species of the inhibitor. In such cases, it is interesting to investigate the preferred species interacting with the metal surface and to study the influence of

protonation on the molecular structures and the molecular properties of the inhibitors. At low pH, the benzothiazoles are protonated. At this pH it carries a net positive charge. Gas phase benzothiazoles exclusively exist in the neutral form. So, to shed light on the effectiveness of the benzothiazoles in acidic media, neutral and protonated forms, both in gas and aqueous phases were used for quantum chemical calculations.

The AIM method (Bader, 1990) provides the opportunity to have an insight into a region of a system. Geometrical, topological and energy parameters are useful tools in characterizing the bond strength. The wave function obtained from the optimization was used to calculate the topological properties such as electron density, Laplacian of electron density and the total energy densities at the Bond critical points (BCP) using the Bader's theory of 'Atoms in Molecules', was implemented in AIM 2000 software (Biegler-Konig & Schonbohm, 2002).

Molecular properties, related to the reactivity and selectivity of the compounds were estimated following the Koopmans's theorem relating the energy of the HOMO and the LUMO (Zhan, Nichols, & Dixon, 2003).

Global hardness ( $\eta$ ) measures the resistance of an atom to a charge transfer (Parr & Weitao, 1989); it is estimated by using the equation:

$$\eta = \frac{1}{2}(E_L - E_H) \quad (1)$$

Electronegativity  $\chi$  is the measure of the power of an atom or group of atoms to attract electrons to it when chemically combined with another atom (Sastri & Perumareddi, 1997); it can be estimated by using the equation:

$$\chi = -\frac{1}{2}(E_L + E_H) \quad (2)$$

During the interaction of the inhibitor molecule with bulk metal, electrons flow from the lower electronegativity molecule to the higher electronegativity metal until the chemical potential becomes equalized. The fraction of the transferred electron,  $\Delta N$ , was estimated through the equation:

$$\Delta N = \frac{\chi_m - \chi_i}{2(\eta_m + \eta_i)} \quad (3)$$

where the indices "m" and "i" refer to metal atom and inhibitor molecule, respectively and where  $\chi_m$  and  $\chi_i$  denote the absolute electronegativity of iron and the inhibitor molecule respectively;  $\eta_m$  and  $\eta_i$  denote the absolute hardness of iron and the inhibitor molecule respectively. The theoretical values of  $\chi_m$  and  $\eta_m$  for bulk iron 7 eVmol<sup>-1</sup> and 0 eVmol<sup>-1</sup> were used respectively by assuming that for a metallic bulk I = A, because they are softer

than the neutral metallic atoms (Khaled, 2010; Pearson, 1988).

The electric dipole polarizability is a measure of the linear response of the electron density in the presence of an infinitesimal electric field  $F$  and it represents a second order variation in energy

$$\alpha = - \left( \frac{\partial^2 E}{\partial^2 F_a \partial^2 F_b} \right)_{a,b=x, y, z} \quad (4)$$

The polarizability  $\alpha$  is calculated as the mean value as given in the following equation:

$$\alpha = \frac{1}{3} (\alpha_{xx} + \alpha_{yy} + \alpha_{zz}) \quad (5)$$

### 3. Result and Discussion

The global molecular reactivity can be studied according to Fukui's theory of frontier molecular orbitals (FMO) in terms of interaction between the frontier orbitals, namely the HOMO and the LUMO (Fukui, 1982).  $E_{\text{HOMO}}$  describes the electron donating ability of the molecule. Therefore, inhibitors with high values of  $E_{\text{HOMO}}$  tend to donate electrons to a proper acceptor with a low empty molecular orbital energy.

The energy of LUMO on the other hand, shows the ability of the molecule to accept electrons. The lower the value of  $E_{\text{LUMO}}$ , the more probable it is that the molecule accepts electrons (Popova, Christov, & Deligeorgiev, 2003).

The inhibition efficiency increases with the increasing  $E_{\text{HOMO}}$  values. High  $E_{\text{HOMO}}$  values indicate that the molecule tends to donate electrons to the appropriate acceptor molecules with a low-energy empty molecular orbital. The lower value of  $E_{\text{LUMO}}$ , suggests the molecule easily accepts electrons from the donor molecules (Ebenso, Arslan, Kandemirli, Caner, & Love, 2010).

Tables 1, 2 and 3 present the calculated values of  $E_{\text{HOMO}}$  and  $E_{\text{LUMO}}$  for the studied benzothiazoles in gas and aqueous phases for the non-protonated and the protonated species. Based on the increasing value of  $E_{\text{HOMO}}$ , the order for the variation of inhibition efficiencies of the studied inhibitors (for both gas and aqueous phases) is consistent with the order obtained from experimental data (TBTA > MBTA > BTA). However, from the results obtained for  $E_{\text{LUMO}}$  in gas and aqueous phases the trend in the  $E_{\text{LUMO}}$  value does not correlate well with the trend in the experimentally determined inhibition efficiency.

Absolute hardness is a very important parameter when describing molecular reactivity and stability. Soft molecules are more reactive than hard ones because they can easily offer electrons. Therefore,

inhibitors with the least values of global hardness are expected to be good corrosion inhibitors for bulk metals in acidic media. According to Wang et al. (Wang, Wang, Wang, Wang, & Liu, 2007), adsorption of inhibitor onto a metallic surface occurs at the part of a molecule which has the greatest softness and lowest hardness. Tables 1, 2 and 3 present the calculated values of  $\eta$  for the studied benzothiazole derivatives in gas and aqueous phases for the non-protonated and the protonated species. The calculations indicate that BTA and MBTA have the highest hardness values compared to TBTA, respectively.

The number of electrons transferred ( $\Delta N$ ) was also calculated and tabulated in Table 1 for the non-protonated, and Tables 2 and 3 for the protonated species. The positive number of electrons transferred ( $\Delta N$ ) indicates that the molecules act as an electron acceptor, while a negative number of electrons transferred ( $\Delta N$ ) indicates that the molecules act as electron donors (El Ashry el, El Nemr, & Ragab, 2012). As can be seen from Table 1, 2 and 3, in aqueous phase all the molecules studied act as electron donors. According to Lukovits's (Lukovits, Kálmán, & Zucchi, 2001) study, if the value of  $\Delta N < 3.6$ , the inhibition efficiency increases along with the increasing electron donating ability of the inhibitor at the metal surface. Also it was observed (Eddy, Ibok, Ebenso, El Nemr, & El Ashry el, 2009) that the higher the value of  $\Delta N$ , the greater the tendency of a molecule to donate electrons to the electron poor species. In the case of corrosion inhibitors, a higher  $\Delta N$  implies a greater tendency to interact with the metal surface (i.e., a greater tendency to adsorb on the metal surface). Values of  $\Delta N$  for the non-protonated species show that TBTA has the highest  $\Delta N$  value in gas phase and in aqueous phase. Values of  $\Delta N$  for the non-protonated species show that  $\Delta N$  values correlate strongly with experimental inhibition efficiencies. Thus, the highest fraction of electrons transferred is associated with the best inhibitor (TBTA), while the least fraction is associated with the inhibitor that has the least inhibition efficiency (BTA). The values of  $\Delta N$  showed that the inhibition efficiency resulting from electron donation is in agreement with Lukovits's study. For the protonated species  $\Delta N$  is Negative in gas phase, which may be related to tendency of the protonated species to Attract electrons from the metal in this phase.  $\Delta N$  of the protonated species is smaller than the non-protonated species in the two phases, which may be related to the decreased tendency of the protonated species to donate electrons.

**Table 1.** Quantum chemical parameters for three benzothiazoles (BTA, MBTA and TBTA) in the non-protonated form, calculated at B3LYP/6311++G\*\* level

		$E_{\text{HOMO}}$ (ev)	$E_{\text{LUMO}}$ (ev)	$\eta$ (ev)	$\Delta N$ (e)	$\alpha$ (a.u.)	Surface area( $\text{\AA}^2$ )	TNC (e)
gas	TBTA	-5.79	-0.77	2.378	0.753	141.98	182.11	-5.0863
	MBT	-5.91	-0.68	2.614	0.707	131.63	181.45	-4.5490
	BTA	-6.10	-1.03	2.662	0.668	116.82	161.29	-3.6133
in water solution	TBTA	-5.825	-0.91	2.456	0.739	200.59	193.31	-5.3048
	MBTA	-6.021	-0.74	2.635	0.685	183.65	190.86	-4.6984
	BTA	-6.178	-0.84	2.665	0.654	164.91	170.32	-3.7501

**Table 2.** Quantum chemical parameters for three benzothiazoles (BTA, MBTA and TBTA), in the protonated form (N9-H) calculated at B3LYP/6311++G\*\* level

		$E_{\text{HOMO}}$ (ev)	$E_{\text{LUMO}}$ (ev)	$\eta$ (ev)	$\Delta N$ (e)	$\alpha$ (a.u.)
gas	TBTA	-9.30	-5.60	1.850	-0.123	137.41
	MBT	-10.25	-5.56	2.340	-0.194	124.91
	BTA	-10.512	-5.73	2.38	-0.235	108.76
in water solution	TBTA	-6.53	-2.01	2.26	0.602	189.58
	MBTA	-7.09	-2.00	2.54	0.481	170.20
	BTA	-7.233	-2.09	2.57	0.454	150.39

**Table 3.** Quantum chemical parameters for three benzothiazoles (BTA, MBTA and TBTA), in the protonated form (N10-H) calculated at B3LYP/6311++G\*\* level

		$E_{\text{HOMO}}$ (ev)	$E_{\text{LUMO}}$ (ev)	$\eta$ (ev)	$\Delta N$ (e)	$\alpha$ (a.u.)
gas	TBTA	-9.543	-5.569	1.850	-0.123	135.37
	MBT	-10.395	-5.496	2.340	-0.194	122.33
	BTA	-10.776	-5.646	2.38	-0.235	107.00
in water solution	TBTA	-6.231	-1.817	2.206	0.674	197.64
	MBTA	-6.823	-1.729	2.546	0.534	180.57
	BTA	-6.919	-1.679	2.61	0.515	168.04

Polarizability ( $\alpha$ ) indicate the polarity of a molecule and this is a good reactivity indicators (Ju, Kai, & Li, 2008). The bigger the value of polarizability, the greater the possibility of the molecule to change its original shape and the better tendency the molecule will have to be absorbed on the metal surface. Polarizability is the ratio of induced dipole moment to the intensity of the electric field. The induced dipole moment is proportional to polarizability (Eddy et al., 2009). Some attempts have been made to relate the polarizability of some corrosion inhibitors to their inhibition efficiency. According to Arslan et al. (Arslan, Kandemirli, Ebenso, Love, & Alemu, 2009), the minimum polarizability principle (MPP) expects that the natural direction of evolution of any system is toward a state of minimum polarizability. The obtained polarizability values for three benzothiazole by using Eq. (5) is shown in Tables 1, 2 and 3 and as can be seen the

trend for the variation of polarizability is TBTA > MBTA > BTA for the non-protonated and the protonated species reveal that the trend of increasing inhibition efficiencies of the inhibitors with respect to increasing polarizability correlates well with the order of the experimental % inhibition efficiencies results (TBTA > MBTA > BTA).

Surface area ( $\text{\AA}^2$ ) provides information about the surface coverage of the metal by the inhibitor molecule. The compound that has large surface area value has the highest surface coverage and hence might give greater protection of the metal surface.

The inhibition efficiency increases as the surface area of the molecules increases due to the increase of the contact area between the molecule and the surface. A comparison of the surface area values across structures show the order TBTA > MBTA > BTA for both gas and aqueous phases, which agrees with the experimentally determined

inhibition efficiency of the compounds. The trend in the surface area values correlate well with the experimentally determined inhibition efficiencies.

According to classical chemical theory, all chemical interactions are either by electrostatic or orbital interactions. Electrical charges in the molecule were obviously the driving force of electrostatic interactions. It is proved that local electric densities or charges are important in many chemical reactions and physicochemical properties of compound (Xia, Qiu, Yu, Liu, & Zhao, 2008).

The partial charges on the individual atoms in a molecule also indicate the reactive centers for a particular inhibitor. The atoms with the highest negative charge are considered to have the highest tendency to donate electrons to the metal surface. Therefore, the inhibitor is likely to interact with the metal surface through such atoms.

The Mulliken atomic charges on the atoms of the studied benzothiazole derivatives in gas and

aqueous phases are summarized in Tables 4, 5 and 6. The negative charge centers could offer electrons to the Fe atoms to form coordinate bonds while the positive charge centers can accept electrons from 3d orbitals of the Fe atom to form feedback bonds, thus further strengthening the interaction of inhibitor and Fe surface. According to the Mulliken atomic charges the most favorable sites for the interaction with the metal surface for non-protonated species were heteroatoms; because these atoms have a larger negative charge, which suggests that those active centers with excess charges could act as a nucleophilic group. The binding capability of the metal on the inhibitor depends strongly on the electronic charge of the active site (Nataraja, Venkatesha, Tandon, & Shylesha, 2011). Each inhibitor molecule was allowed to interact with the Fe metal at the atom that has the highest negative charge.

**Table 4.** The calculated atomic charges for the non-protonated BTA inhibitor in gas phase and solution

BTA	gas	in water solution	MBTA	gas	in water solution	TBTA	gas	in water solution
1 C	-1.6311	-1.5048	1 C	-1.418	-1.3119	1 C	-1.618	-1.452
2 C	2.0586	2.0305	2 C	2.2863	2.2452	2 C	2.681	2.785
3 C	0.0703	0.0259	3 C	-0.771	-0.8094	3 C	-0.936	-1.029
4 C	-0.1257	-0.1741	4 C	0.5282	0.5060	4 C	0.965	0.592
5 C	-0.3145	-0.3621	5 C	-0.102	-0.1525	5 C	-0.034	0.214
6 C	-0.8313	-0.8699	6 C	-0.975	-1.0141	6 C	-1.192	-1.265
7 C	0.2954	0.3279	7 C	0.2643	0.29881	7 C	0.3085	0.360
8 S	-0.4399	-0.4413	8 S	-0.516	-0.5053	8 S	-0.453	-0.459
9 N	-0.2611	-0.3065	9 N	-0.256	-0.3009	9 N	-0.259	-0.3052
10 N	-0.0095	-0.0910	10 N	-0.012	-0.0947	10 N	-0.003	-0.0820
11 H	0.1655	0.2023	11 H	0.1768	0.1921	11 H	0.1857	0.2071
12 H	0.1799	0.1957	12 H	0.1630	0.1907	12 H	0.1961	0.1904
13 H	0.1634	0.1912	13 H	0.2679	0.2917	13 H	0.2692	0.2939
14 H	0.1595	0.1886	14 H	0.2494	0.2897	14 H	0.2537	0.2933
14 H	0.2675	0.2930	15 H	0.1558	0.1951	15 H	0.1918	0.2304
15 H	0.2527	0.2946	16 C	-0.499	-0.5093	16 S	-0.592	-0.7102
			17 H	0.1486	0.1598	17 H	0.0384	0.1367
			18 H	0.1565	0.1636			
			19 H	0.1583	0.1653			

Another parameter that was considered and that can provide valuable information about the reactive behavior of the studied inhibitors is the total negative charge (TNC) obtained by summing up all the negative charges within a molecule (Masoud, Awad, Shaker, & El-Tahawy, 2010; Nataraja et al., 2012). Summation of the total negative charges on atoms over the skeleton of the molecule (TNC) is collected in Tables 4, 5 and 6. The calculations showed that in two phases the inhibitor with the highest inhibition efficiency has the highest TNC value which agrees well with the experimental observations.

The frontier orbitals electron density distributions are of great importance in describing the adsorption preference of the inhibitors. The calculated HOMO electron density distributions of the three inhibitors for the non-protonated species in two phases in Figs. 2 and 3 are presented. In BTA and MBTA, the

HOMO is strongly localized on C1, C2, N10, C6, C5 and S8 atoms while the LUMO is spread out almost on benzene ring and C7, N9 atoms. In TBTA, the HOMO is spread on the benzene ring and N10, N9, C7 atoms, especially in the S16 atom which implies that these are the regions of the molecule with the highest tendency to donate electrons while the LUMO is strongly localized on benzene ring and C7, N9 atoms of the thiazole ring.

Molecules of BTA and MBTA inhibitors can be directly adsorbed at the steel surface on the basis of donor– acceptor interactions between  $\pi$ -electrons of benzene ring, on bonding lone pairs of S6 and N9 atoms, and vacant d-orbitals of iron atoms.

Molecular electrostatic potential (MEP) contour map reflects the electronic density distributions within the molecule, the MEP contour map of the compound is shown in Figs. 2 and 3. Red and blue areas in the MEP map refer to the regions of negative and positive potentials and correspond to

the electron-rich and electron-poor regions, respectively, whereas the green color signifies the neutral electrostatic potential. It can be seen that the negatively charged regions are the benzene ring and N10 atom. These electron-rich areas would be the preferred sites for adsorption to metal surfaces.

Benzothiazole can be easily protonated in an acidic medium. All possibilities of protonation at the active centers (N9 and N10 atoms) of the investigated compounds were calculated. It is shown that the protonation at N10 atom is favored.

This was confirmed by calculating the total energy for the protonated system that gives the lowest energy on protonation at N10 and N9 atoms.

The extent of protonation (i.e., how likely the molecule would prefer to be protonated) is estimated using the proton affinity (PA) of the inhibitors. The proton affinity is obtained using the equation:

$$PA = E_{\text{prot}} + E_{\text{H}_2\text{O}} - E_{\text{non-prot}} - E_{\text{H}_3\text{O}^+} \quad (6)$$

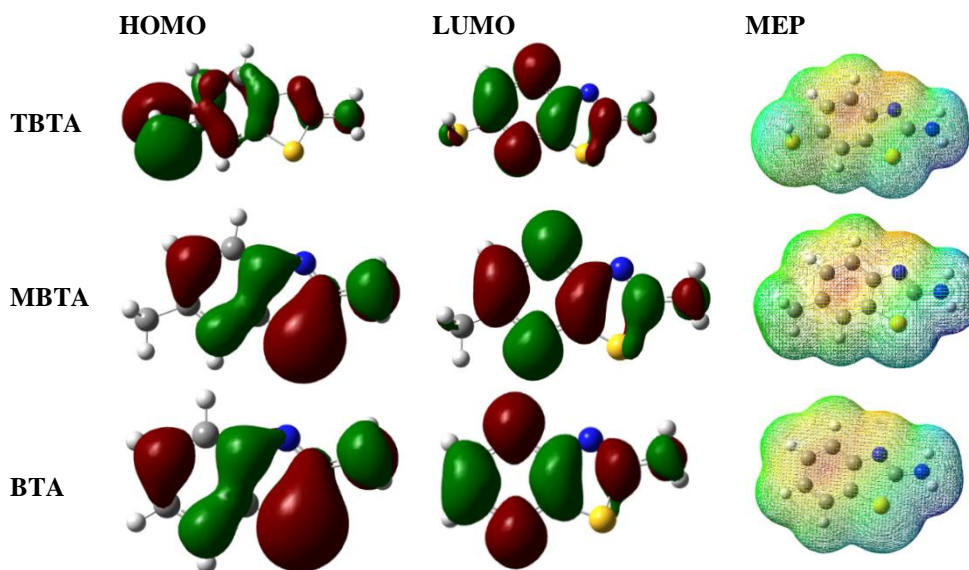


**Fig. 2.** The frontier molecule orbital density distribution for three benzothiazoles (BTA, MBTA and TBTA) in the non-protonated form in gas phase: (a) HOMO, (b) LUMO, (c) molecular electrostatic potential contour map (MPE), respectively (Red: Strong negative electrostatic potential (EP); Blue: Strong positive EP; Green: Moderately positive EP)

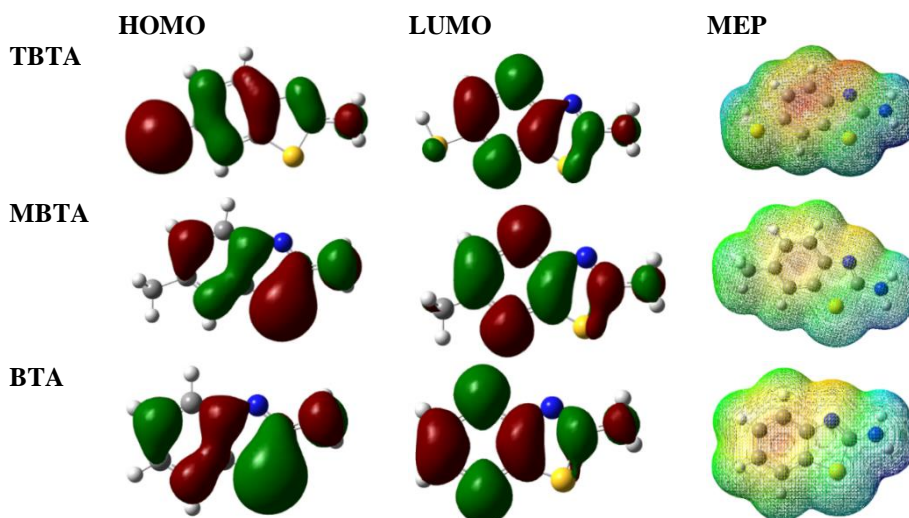


**Fig. 3.** The frontier molecule orbital density distribution for three benzothiazoles (BTA, MBTA and TBTA) in the non-protonated form in solution: (a) HOMO, (b) LUMO, (c) molecular electrostatic potential contour map (MPE), respectively (Red: Strong negative electrostatic potential (EP); Blue: Strong positive EP; Green: Moderately positive EP)

where  $E_{\text{prot}}$  and  $E_{\text{non-prot}}$  are the total energies of the protonated and the neutral (non-protonated) inhibitors respectively,  $E_{\text{H}_2\text{O}}$  is the total energy of a water molecule and  $E_{\text{H}_3\text{O}^+}$  is the total energy of the hydronium ion.

Results from Table 7 and 8 suggest that protonation on the N10 atom are preferred to the N9 atom. The calculations show that the protonation process is an exothermic reaction, which means that all inhibitors have a considerable tendency for protonation in acidic medium.

In the case of Fe surface, the inhibitor-metal interaction mechanism may be modelled by placing a Fe atom in the vicinity of the electron-donor centers (i.e., chelating or active adsorption sites) and optimizing the resulting geometry. Although the inhibitor-Fe interaction energy obtained from this model does not reflect the real interaction energy between the inhibitor and the Fe surface (which contains many Fe atoms), it is nevertheless a good model for qualitative analysis of the type of interactions involved and a good indication of the inhibitor-Fe interaction strength for different electron donor sites (active adsorption sites) on the inhibitor molecule.

In order to investigate the spontaneity of this adsorption process, the thermodynamic parameter, Gibb's free energy change,  $\Delta G$ , is calculated using

$$\Delta G = \Delta H - T\Delta S \quad (7)$$

where  $\Delta G$  is the free energy change,  $\Delta H$  is the enthalpy change,  $\Delta S$  is the entropy change, and  $T$  is the absolute temperature. Figures 4 and 5 present the optimized Fe-inhibitor complexes, and the calculated enthalpy, entropies and Gibbs free energy changes in the formation processes of the Fe-inhibitor complexes are tabulated in Tables 9, 10. The adsorption process is performed at room temperature. Obviously, for the enthalpy changes ( $\Delta H$ ) suggest that the formation processes of the Fe-inhibitor complexes are an exothermic reaction. Moreover, for the formation of Fe-TBTA complex the heat released from it is much larger than the formations of the other two complexes. As for the Gibbs free energy changes ( $\Delta G$ ) the formation processes involving the TBTA, MBTA, and BTA are negative values. Therefore, the formations of these three Fe-inhibitor complexes are spontaneous at 298.15 K and 1.0 atm. Hence, for a good corrosion inhibitor, its interaction with Fe metal should be favorable thermodynamically.

**Table 7.** The calculated proton affinity (PA) and total energy of (Inhibitor+H(N9-H)) for three benzothiazoles (BTA, MBTA and TBTA) respectively in both media

		$E_{(\text{Inhibitor}+\text{H})}$ (Kcal)	PA(Kcal)
gas	TBTA(N9-H)	-738398.075	-36.534
	MBT(N9-H)	-513202.705	-38.716
	BTA(N9-H)	-488522.801	-36.489
in water solution	TBTA(N9-H)	-738461.452	-11.730
	MBT(N9-H)	-513260.487	-12.422
	BTA(N9-H)	-488581.540	-11.609

**Table 8.** The calculated proton affinity (PA) and total energy of (Inhibitor+H(N10-H)) for three benzothiazoles (BTA, MBTA and TBTA) respectively in both media

		$E_{(\text{Inhibitor}+\text{H})}$ (Kcal)	PA(Kcal)
gas	TBTA(N10-H)	-738426.312	-61.634
	MBT(N10-H)	-513228.416	-64.426
	BTA(N10-H)	-488548.750	-62.439
in water solution	TBTA(N10-H)	-738479.022	-29.145
	MBT(N10-H)	-513278.057	-30.292
	BTA(N10-H)	-488599.737	-29.642

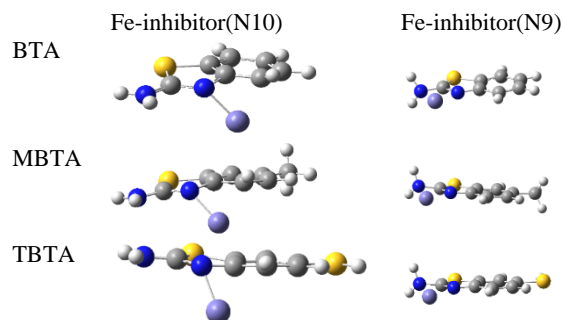


**Fig. 4.** Optimized inhibitor-metal complexes for the investigated three benzothiazoles (BTA, MBTA and TBTA) respectively

According to Sahin et al. (Şahin, Gece, Karıcı, & Bilgiç, 2008), the strength of the interaction between the metal and the inhibitors was then estimated as the difference between when the adsorption occurs between the inhibitor and Fe, the energy of the new system is expressed as ( $E_{\text{Fe-X}}$ ) and the sum of the total energy of the iron atom and isolated inhibitor ( $E_{\text{X}} + E_{\text{Fe}}$ ) resulted in the equation;

$$E_{\text{int}} = E_{(\text{Fe-X})} - (E_{\text{X}} + E_{\text{Fe}}) \quad (8)$$

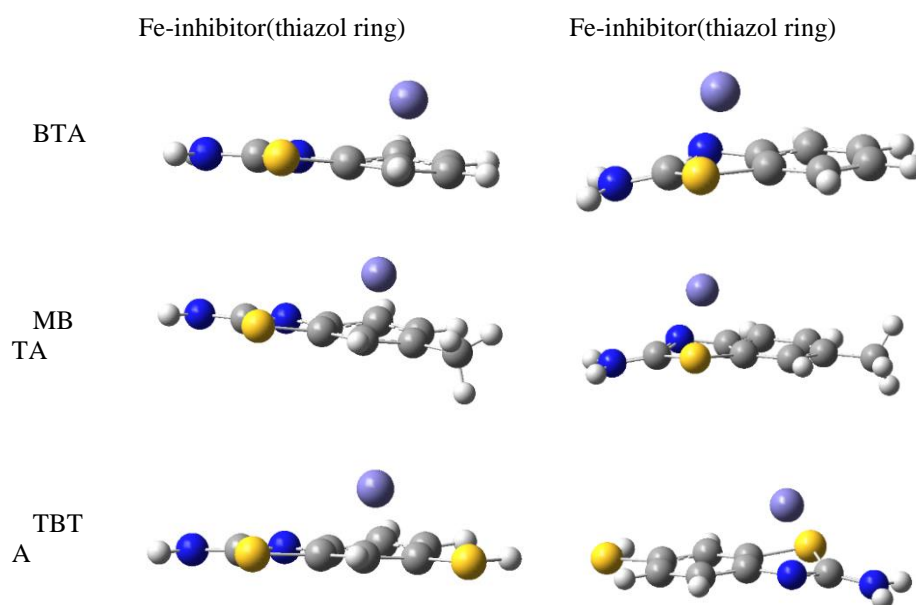


**Fig. 5.** Optimized inhibitor-metal complexes for the investigated three benzothiazoles (BTA, MBTA and TBTA) respectively

**Table 9.** Calculated enthalpies changes ( $\Delta H(\text{J mol}^{-1})$ ), entropies changes ( $\Delta S(\text{J mol}^{-1} \text{K}^{-1})$ ) and free energy changes ( $\Delta G(\text{J mol}^{-1})$ ) of the studied benzothiazole derivatives (BTA, MBTA and TBTA), respectively, and Fe system in gas phase

	( $\Delta S$ )	( $\Delta H$ )	( $\Delta G$ )
TBTA(N9+Fe)	-0.1338	-1284.0744	-1244.1771
MBTA(N9+Fe)	-0.1246	-1238.0213	-1200.8619
BTA(N9+Fe)	-0.1209	-1210.2229	-1174.1670
TBTA(N10+Fe)	-0.1380	-1240.2739	-1242.9302
MBTA(N10+Fe)	-0.1224	-1272.4752	-1235.9841
BTA(N10+Fe)	-0.1256	-1238.8010	-1201.3524
TBTA(thiazol ring+Fe)	-0.1346	-1257.4969	-1217.3776
MBTA(thiazol ring+Fe)	-0.1309	-1253.0310	-1214.0089
BTA(thiazol ring+Fe)	-0.1261	-1220.1051	-1182.5131
TBTA(benzene ring+Fe)	-0.1422	-1318.0505	-1275.6857
MBTA(benzene ring+Fe)	-0.1421	-1315.9922	-1273.6448
BTA(benzene ring+Fe)	-0.1317	-1278.9338	-1239.6835

In Fe–inhibitor (TBTA) complex, the charges on Fe ion decreases which suggests that charge has been transferred to the metal ion. This decrease in the charge density may be related to the charge transfer from the inhibitor to the metal surface. In this way, charge transfer mechanism is the most probable mode of interaction between the metal and the inhibitor molecule.

**Table 10.** Calculated enthalpies changes ( $\Delta H(\text{J mol}^{-1})$ ), entropies changes ( $\Delta S(\text{J mol}^{-1} \text{K}^{-1})$ ) and free energy changes ( $\Delta G(\text{J mol}^{-1})$ ) of the studied benzothiazole derivatives (BTA, MBTA and TBTA), respectively, and Fe system in water solution

	( $\Delta S$ )	( $\Delta H$ )	( $\Delta G$ )
TBTA(N9+Fe)	-0.1354	-253.9043	-217.0592
MBTA(N9+Fe)	-0.1259	-242.9588	-205.4316
BTA(N9+Fe)	-0.1402	-240.7298	-198.9335
TBTA(N10+Fe)	-0.1236	-239.1387	-198.7738
MBTA(N10+Fe)	-0.1178	-214.2310	-179.1152
BTA(N10+Fe)	-0.1193	-208.6519	-173.0985
TBTA(thiazol ring+Fe)	-0.1348	-185.9128	-145.7349
MBTA(thiazol ring+Fe)	-0.1298	-183.2401	-144.5471
BTA(thiazol ring+Fe)	-0.1242	-174.4763	-137.4578
TBTA(benzene ring+Fe)	-0.1455	-245.5974	-202.2363
MBTA(benzene ring+Fe)	-0.1423	-243.5731	-201.1447
BTA(benzene ring+Fe)	-0.1302	-228.7839	-189.9551

In Fe–inhibitor (MBTA) complex, the partial atomic charge on Fe atom decreases and the amount of charge transferred to iron is lower than the amount of charge transferred to Fe ion when interacting with TBTA. Charge on the Fe atom in Fe–inhibitor (BTA) complex in comparison with the isolated  $\text{Fe}^{2+}$  ion decreases, suggesting the amount of charge transferred from the inhibitor to iron. Values of  $E_{\text{int}}$  are negative for three inhibitors implying that the adsorption on mild steel surface is spontaneous. Also, from a thermodynamic viewpoint, every system prefers the lowest energy state. Therefore, the lower the values of  $E_{\text{int}}$ , the more stable the formed complex is expected to be. Both results (the interaction energy and the charges on Fe ion) therefore imply that TBTA bind strongly to the metal surface.

To further clarify the nature of the interaction for the Fe–inhibitor we use the Bader's theory of Atoms-in-Molecules (AIMs) which involves topological analysis of electron density between two interacting atoms. According to this theory, atoms that are chemically bonded have their nuclei linked by a (single) bond path (a single line of locally maximum electron density) and they share a bond critical point (a point on the bond path with the lowest value of the electron density). Bond critical point (BCP) is used in the recognition of chemical bonds and strength between atoms. Chemical bonding interactions are characterized

and classified according to the properties of the electron density at the BCP ( $\rho_{\text{bcp}}$ ), its Laplacian ( $\Delta^2\rho_{\text{bcp}}$ ) and the total energy densities ( $H_{\text{bcp}}$ ). The Laplacian of the electron density measures local electron concentration  $\Delta^2\rho_{\text{bcp}} < 0$  and depletion  $\Delta^2\rho_{\text{bcp}} > 0$  within a molecular system. Laplacian of electron density ( $\Delta^2\rho_{\text{bcp}}$ ) is related to the energy of bond interaction by the local expression of the virial theorem (Koch & Popelier, 1995) and additionally to total electron energy density  $H_{\text{bcp}}$  (Matta & Boyd, 2007).

From the sign and magnitude of the Laplacian of  $\rho_{\text{bcp}}$  at the bond critical point it can be determined whether the electronic charge is locally concentrated or depleted. When  $\Delta^2\rho_{\text{bcp}} < 0$ , it indicates that the electronic charge is concentrated in the internuclear region. This is the case in an electron-sharing (or covalent) interaction (Bader, 1998). On the other hand  $\Delta^2\rho_{\text{bcp}} > 0$  shows a depletion of the electronic charge along the bond. This is the case in a closed-shell electrostatic interaction; consequently the bond is polar or ionic. The calculated topological parameters of these complexes are given in Tables 11 and 12. The  $\rho_{\text{bcp}}$  values for parallel configurations were higher than that in direct configuration, showing a more effective interaction in this case.

Moreover, the highest value of  $\rho_{\text{bcp}}$  could be observed in TBTA. According to  $\rho_{\text{bcp}}$  data (Tables

12 and 13) in all complexes the bond strengths around central Fe- atom increase in order. Negative  $\Delta^2\rho_{bcp}$  values of remaining bonds indicate a concentration of electron density in the internuclear region and, consequently, are in agreement with covalent (sharing) character. The interaction between Fe and the active sites of inhibitors can be confirmed by existence of BCP of the Fe- complex contact. As mentioned above, the electron density  $\rho_{bcp}$  can be used to characterize the relative strength of the Fe- inhibitor contact. For example, the relative order of the  $\rho_{bcp}$  for the three Fe–inhibitor complexes is: Fe–TBTA > Fe–MBTA > Fe–BTA, which is also consistent with the relative order of the Fe–inhibitor contact distance shown in Tables 12 and 13. The sign of  $H_{bcp}$  determines

whether the accumulation of charge at a given point is stabilizing ( $H_{bcp} > 0$ ) or destabilizing ( $H_{bcp} < 0$ ). The calculated values of  $H_{bcp}$  reported for BCPs in complexes are given in Tables 12 and 13. The values  $H_{bcp}$  are all positive, which implies a stabilizing effect due to the depleting charge in the bond region and the presence of electrostatic interaction. The results show that the interaction between Fe and the active sites of inhibitors are related to partially covalent and partially electrostatic bond ( $\Delta^2\rho_{bcp} < 0$  and  $H_{bcp} > 0$ ).

**Table 11.** Calculated results of interaction energies ( $E_{int}$ (Kcal)) between the metal and the inhibitor atom, and the charges on Fe in inhibitor-metal complexes in gas and water solution phases for three benzothiazole derivatives (BTA, MBTA and TBTA), respectively

	$E_{int}$	charges on Fe	$E_{int}$	charges on Fe
	gas		in water	solution
TBTA(N9+Fe)	-238.1114	0.914	-365.2335	1.332
MBTA(N9+Fe)	-235.0425	0.939	-358.9727	1.368
BTA(N9+Fe)	-227.2540	1.007	-239.5154	1.420
TBTA(N10+Fe)	-226.9958	0.611	-368.6271	1.491
MBTA(N10+Fe)	-226.1444	0.636	-366.1493	1.510
BTA(N10+Fe)	-219.6824	0.662	-232.0254	1.520
TBTA(thiazol ring+Fe)	-230.9789	0.496	-349.6700	0.929
MBTA(thiazol ring+Fe)	-229.6523	0.536	-344.0768	0.934
BTA(thiazol ring+Fe)	-221.9693	0.549	-223.3524	0.954
TBTA(benzene ring+Fe)	-244.4673	0.460	-371.8103	0.855
MBTA(benzene ring+Fe)	-243.2478	0.492	-365.7748	0.865
BTA(benzene ring+Fe)	-236.4326	0.510	-236.6604	0.879

A comparison of the molecular properties of the inhibitors between the results in vacuo and the results in water solution provides a gauge of the effect of the solvent on molecular properties.

From the computed results, in gas and aqueous phases, the stabilization effect of the solvent is mainly noticed in the increase of all total negative charges on atoms with respect to gas phase.

Another noteworthy solvent effect is the increase of the polarizability values in solution, which is probably a result of the polarization of the inhibitor molecules by the solvent, leading to an increase in the charge separation in the molecules. The

stabilization effect is also observed in the increase of charges of atoms which indicate a higher disposition of the inhibitors to donate their electrons; hence a better adsorption onto the mild steel surface.

**Table 12.** The calculated topological parameters at the BCPs of the Fe-X (X = N9, N10, thiazol ring and benzene ring) contact in the Fe–inhibitor complexes studied and the bond distance of the Fe-X (X = N9, N10, thiazol ring and benzene ring) in gas phase for three benzothiazole derivatives (BTA, MBTA and TBTA), respectively

	$\rho_{bcp}(e/\text{\AA}^3)$	$\Delta^2\rho_{bcp}(e/\text{\AA}^5)$	$H_{bcp}(e/\text{\AA}^4)$	bond distance( $\text{\AA}$ )
TBTA(N9+Fe)	0.0952	-0.0980	0.0280	2.001
MBTA(N9+Fe)	0.0929	-0.0980	0.0191	2.007
BTA(N9+Fe)	0.0897	-0.0975	0.0170	2.009
TBTA(N10+Fe)	0.1130	-0.1073	0.0302	1.910
MBTA(N10+Fe)	0.1061	-0.0992	0.0258	1.943
BTA(N10+Fe)	0.1056	-0.0980	0.0255	1.944
TBTA(thiazol ring+Fe(Fe+S))	0.0643	-0.0466	0.0131	2.342
TBTA(thiazol ring+Fe(Fe+N10))	0.0911	-0.0973	0.0173	1.998
TBTA(thiazol ring+Fe(Fe+C1))	0.0826	-0.0698	0.0187	2.069
MBTA(thiazol ring+Fe(Fe+S))	0.0679	-0.0488	0.0143	2.319
MBTA(thiazol ring+Fe(Fe+N10))	0.0870	-0.0919	0.0153	2.020
MBTA(thiazol ring+Fe(Fe+C1))	0.0809	-0.0649	0.0188	2.079
BTA(thiazol ring+Fe(Fe+S))	0.0690	-0.0493	0.0145	2.315
BTA(thiazol ring+Fe(Fe+N10))	0.0857	-0.0895	0.0148	2.026
BTA(thiazol ring+Fe(Fe+C1))	0.0691	-0.056	0.0165	2.093
TBTA(benzene ring+Fe (Fe+C2))	0.0812	-0.0588	0.0189	2.101
TBTA(benzene ring+Fe (Fe+C3))	0.0852	-0.0612	0.0210	2.064
TBTA(benzene ring+Fe (Fe+C5))	0.0829	-0.0579	0.0202	2.078
MBTA(benzene ring+Fe(Fe+C3))	0.0847	-0.0592	0.0206	2.073
MBTA(benzene ring+Fe(Fe+C4))	0.0818	-0.0579	0.0186	2.103
MBTA(benzene ring+Fe(Fe+C5))	0.0816	-0.0576	0.0190	2.092
BTA(benzene ring+Fe(Fe+C3))	0.0834	-0.0598	0.0194	2.086
BTA(benzene ring+Fe(Fe+C4))	0.0842	-0.0631	0.0198	2.073

It can be concluded from the results of most of the global descriptors in gas and aqueous phases that TBTA is the best inhibitor among the three studied molecules; these parameters give information on the chemical reactivity of the studied molecules in gas and aqueous phases. Trends in the quantum chemical parameters are similar for the results in vacuo and in water solution.

Accordingly the classification of these three inhibitors based on the theoretical study is in quite a good agreement with the reported experimental

corrosion inhibition efficiencies (Patel et al., 2014).

A comparison of the molecular properties between the protonated and the non-protonated species of the individual structures shows that the protonated form has lower  $E_{\text{HOMO}}$ , higher  $E_{\text{LUMO}}$ , lower polarizability and lower  $\Delta N$ , which suggests that protonation decreases the tendency of an inhibitor to donate electrons.

**Table 13.** The calculated topological parameters at the BCPs of the Fe-X (X = N9, N10, thiazol ring and benzene ring) contact in the Fe–inhibitor complexes studied and the bond distance of the Fe-X (X = N9, N10, thiazol ring and benzene ring) in water solution for three benzothiazole derivatives (BTA, MBTA and TBTA), respectively

	$\rho_{bcp}(e/\text{\AA}^3)$	$\Delta^2\rho_{bcp}(e/\text{\AA}^5)$	$H_{bcp}(e/\text{\AA}^4)$	bond distance(\text{\AA})
TBTA(N9+Fe)	0.0846	-0.0956	0.0137	2.001
MBTA(N9+Fe)	0.0845	-0.0972	0.0136	2.012
BTA(N9+Fe)	0.0825	-0.0981	0.0124	1.943
TBTA(N10+Fe)	0.0952	-0.1188	0.0180	1.910
MBTA(N10+Fe)	0.0975	-0.1038	0.0203	1.957
BTA(N10+Fe)	0.1023	-0.1026	0.0235	1.944
TBTA(thiazol ring+Fe(Fe+S))	0.0585	-0.0446	0.0100	2.378
TBTA(thiazol ring+Fe(Fe+N10))	0.0723	-0.0824	0.0072	2.089
TBTA(thiazol ring+Fe(Fe+C1))	0.0725	-0.0600	0.0145	2.121
MBTA(thiazol ring+Fe(Fe+S))	0.0592	-0.0451	0.0101	2.375
MBTA(thiazol ring+Fe(Fe+N10))	0.0710	-0.0804	0.0068	2.097
MBTA(thiazol ring+Fe(Fe+C1))	0.0716	-0.0591	0.0142	2.128
BTA(thiazol ring+Fe(Fe+S))	0.0591	-0.0450	0.0100	2.376
BTA(thiazol ring+Fe(Fe+N10))	0.0707	-0.0800	0.0067	2.096
BTA(thiazol ring+Fe(Fe+C1))	0.0685	-0.0589	0.0121	2.152
TBTA(benzene ring+Fe (Fe+C2))	0.0770	-0.0634	0.0152	2.083
TBTA(benzene ring+Fe (Fe+C3))	0.0809	-0.0624	0.0177	2.128
TBTA(benzene ring+Fe (Fe+C5))	0.0786	-0.0600	0.0167	2.099
MBTA(benzene ring+Fe(Fe+C3))	0.0816	-0.0616	0.0179	2.083
MBTA(benzene ring+Fe(Fe+C4))	0.0797	-0.0625	0.0165	2.103
MBTA(benzene ring+Fe(Fe+C5))	0.0800	-0.0602	0.0172	2.096
BTA(benzene ring+Fe(Fe+C3))	0.0808	-0.06215	0.0172	2.090
BTA(benzene ring+Fe(Fe+C4))	0.0805	-0.0648	0.0167	2.088
BTA(benzene ring+Fe(Fe+C5))	0.0776	-0.0619	0.0152	2.114

#### 4. Conclusion

The results of DFT calculations on three benzothiazole (BTA, MBTA and TBTA) have been presented in vacuo and in water solution, taking into account both the non-protonated and protonated species. The experimental inhibition efficiencies are closely related to the quantum chemical parameters such as  $E_{\text{HOMO}}$ ,  $\eta$ ,  $\Delta N$ , total negative charges,  $\alpha$  and Surface area. A comparison of the results in gas phase and in aqueous phases

shows that trends in the molecular properties are similar. The solvent effect was clearly detected in the stabilization of the inhibitors.

As comparing the TBTA with the other inhibitors, it exhibits a better electrophilic character; the highest  $E_{\text{HOMO}}$ , hence underlining its good ability as an electro-donator. The BTA has the largest hardness and therefore a favorable back-donation charge. These results were found for both phases, namely with and without solvent effect.

Comparison of the protonated species and the non-protonated species show that the protonated

species are more electron deficient than the non-protonated species. Quantum chemical calculations on the Fe-inhibitor complex also reveal that TBTA tends to form the most stable complex and therefore as an inhibitor has the highest tendency to adsorb strongly onto the metal surface. Atoms-in-Molecule (AIM) methods suggest that the Fe-inhibitor interactions in these compounds are partially covalent and electrostatic characters. The frontier orbitals electron density distributions, together with the charge distribution and MEP, predict that all species possess more than one attack center which enables multicenter adsorption of the inhibitor molecules on a metal surface.

### Acknowledgement

We gratefully acknowledge the financial support from the Research Council of the University of Sistan and Baluchestan.

### References

- Al-Mayout, A. M., Al-Suhybani, A. A., & Al-Ameery, A. K. (1998). Corrosion inhibition of 304SS in sulfuric acid solutions by 2-methyl benzoazole derivatives. *Desalination*, 116(1), 25–33.
- Arslan, T., Kandemirli, F., Ebenso, E. E., Love, I., & Alemu, H. (2009). Quantum chemical studies on the corrosion inhibition of some sulphonamides on mild steel in acidic medium. *Corrosion Science*, 51(1), 35–47.
- Bader, R. F. W. (1990). *Atoms in molecules: a quantum theory*, Oxford University, New York.
- Bader, R. F. W. (1998). A Bond Path: A Universal Indicator of Bonded Interactions. *The Journal of Physical Chemistry A*, 102(37), 7314–7323.
- Becke, A. D. (1988). Density-functional exchange-energy approximation with correct asymptotic behavior. *Phys. Rev. A*, 38(6), 3098–3100.
- Becke, A. D. (1993). Density-functional thermochemistry. III. The role of exact exchange. *J. of Chem. Phys.*, 98(7), 5648–5652.
- Biegler-Konig, F., & Schonbohm, J. (2002). Update of the AIM2000-program for atoms in molecules. *J. of Comput. Chem.*, 23(15), 1489–1494.
- Ebenso, E. E., Arslan, T., Kandemirli, F., Caner, N., & Love, I. (2010). Quantum chemical studies of some rhodanine azosulpha drugs as corrosion inhibitors for mild steel in acidic medium. *International Journal of Quantum Chemistry*, 110(5), 1003–1018.
- Eddy, N. O., Ibok, U. J., Ebenso, E. E., El Nemr, A., & El Ashry el, S. H. (2009). Quantum chemical study of the inhibition of the corrosion of mild steel in H<sub>2</sub>SO<sub>4</sub> by some antibiotics. *Molecular Modeling Annual*, 15(9), 1085–1092.
- El Ashry el, S. H., El Nemr, A., & Ragab, S. (2012). Quantitative structure activity relationships of some pyridine derivatives as corrosion inhibitors of steel in acidic medium. *Molecular Modeling Annual*, 18(3), 1173–1188.
- Ergun, Ü., Yüzer, D., & Emregül, K. C. (2008). The inhibitory effect of bis-2,6-(3,5-dimethylpyrazolyl)pyridine on the corrosion behaviour of mild steel in HCl solution. *Materials Chemistry and Physics*, 109(2–3), 492–499.
- Frisch, M. J. T., Schlegel, H. B.; Scuseria, G. E.; Robb, M. A., Cheeseman, J. R.; Montgomery, Jr., J. A., Vreven, T., Kudin, K. N., Burant, J. C., Millam, J. M., Iyengar, S. S., Tomasi, J., Barone, V., Mennucci, B., Cossi, M., Scalmani, G., Rega, N., Petersson, G. A., Nakatsuji, H., Hada, M., Ehara, M., Toyota, K., Fukuda, R., Hasegawa, J., Ishida, M., Nakajima, T., Honda, Y., Kitao, O., Nakai, H., Klene, M., Li, X., Knox, J. E., Hratchian, H. P., Cross, J. B., Bakken, V., Adamo, C., Jaramillo, J., Gomperts, R., Stratmann, R. E.; Yazyev, O.; Austin, A. J., Cammi, R.; Pomelli, C., Ochterski, J. W., Ayala, P. Y., Morokuma, K., Voth, G. A.; Salvador, P.; Dannenberg, J. J., Zakrzewski, V. G.; Dapprich, S., Daniels, A. D., Strain, M. C., Farkas, O.; Malick, D. K., Rabuck, A. D., Raghavachari, K., Foresman, J. B., Ortiz, J. V., Cui, Q., Baboul, A. G., Clifford, S., Cioslowski, J., Stefanov, B. B., Liu, G., Liashenko, A., Piskorz, P., Komaromi, I.; Martin, R. L., Fox, D. J., Keith, T., Al-Laham, M. A., Peng, C. Y.; Nanayakkara, A., Challacombe, M., Gill, P. M. W., Johnson, B., Chen, W., Wong, M. W., Gonzalez, C., and Pople, J. A. (2004). *Gaussian 03, Revision C.02*(Gaussian, Inc., Wallingford CT).
- Fukui, K. (1982). The Role of Frontier Orbitals in Chemical Reactions (Nobel Lecture). *Angewandte Chemie International Edition in English*, 21(11), 801–809.
- Gopi, D., Govindaraju, K. M., & Kavitha, L. (2010). Investigation of triazole derived Schiff bases as corrosion inhibitors for mild steel in hydrochloric acid medium. *Journal of Applied Electrochemistry*, 40(7), 1349–1356.
- Ju, H., Kai, Z.-P., & Li, Y. (2008). Aminic nitrogen-bearing polydentate Schiff base compounds as corrosion inhibitors for iron in acidic media: A quantum chemical calculation. *Corrosion Science*, 50(3), 865–871.
- Khaled, K. F. (2010). Studies of iron corrosion inhibition using chemical, electrochemical and computer simulation techniques. *Electrochimica Acta*, 55(22), 6523–6532.
- Koch, U., & Popelier, P. L. A. (1995). Characterization of C-H-O Hydrogen Bonds on the Basis of the Charge Density. *The Journal of Physical Chemistry*, 99(24), 9747–9754.
- Lee, C., Yang, W., & Parr, R. G. (1988). Development of the Colle-Salvetti correlation-energy formula into a functional of the electron density. *Phys. Rev. B Condens. Matter*, 37(2), 785–789.
- Lukovits, I., Kálmán, E., & Zucchi, F. (2001). Corrosion Inhibitors—Correlation between Electronic Structure and Efficiency. *Corrosion*, 57(1), 3–8.
- Masoud, M. S., Awad, M. K., Shaker, M. A., & El-Tahawy, M. M. T. (2010). The role of structural chemistry in the inhibitive performance of some aminopyrimidines on the corrosion of steel. *Corrosion Science*, 52(7), 2387–2396.
- Matta, C. F., & Boyd, R. J. (2007). *An introduction to the*

- Quantum Theory of Atoms in Molecules*, Wiley-VCH Verlag GmbH.
- Patel, N. S., Beranek, P., Nebyla, M., Pribyl, M., & Šnita, D. (2014). Inhibitive Effects by Some Benzothiazole Derivatives on Mild Steel Corrosion in 1 N HCl. *Int. J. Electrochem. Sci.*, 9, 3951–3960.
- Nataraja, S. E., Venkatesha, T. V., & Tandon, H. C. (2012). Computational and experimental evaluation of the acid corrosion inhibition of steel by tacrine. *Corrosion Science*, 60(0), 214–223.
- Nataraja, S. E., Venkatesha, T. V., Tandon, H. C., & Shylesha, B. S. (2011). Quantum chemical and experimental characterization of the effect of ziprasidone on the corrosion inhibition of steel in acid media. *Corrosion Science*, 53(12), 4109–4117.
- Parr, R. G., & Weitao, Y. (1989). *Density Functional Theory of Atoms and Molecules*, (Oxford University Press, Oxford).
- Pearson, R. G. (1988). Absolute electronegativity and hardness: application to inorganic chemistry. *Inorg. Chem.*, 27(4), 734–740.
- Popova, A., Christov, M., & Deligeorgiev, T. (2003). Influence of the Molecular Structure on the Inhibitor Properties of Benzimidazole Derivatives on Mild Steel Corrosion in 1 M Hydrochloric Acid. *Corrosion*, 59(9), 756–764.
- Quraishi, M. A., Ansari, M. Q., Ahmad, S., & Venkatachari, G. (1998). Influence of some multifunctional triazoles on corrosion of mild-steel in boiling hydrochloric acid solutions. *Bulletin of Electrochemistry.*, 14(10), 302.
- Quraishi, M. A., Wajid Khan, M. A., Ajmal, M., Muralidharan, S., & Venkatakrishna Iyer, S. (1996). Influence of substituted benzothiazoles on corrosion in acid solution. *Journal of Applied Electrochemistry*, 26(12), 1253–1258.
- Rodríguez-Valdez, L. M., Martínez-Villafañe, A., & Glossman-Mitnik, D. (2005). CHIH-DFT theoretical study of isomeric thiazotriazoles and their potential activity as corrosion inhibitors. *Journal of Molecular Structure: THEOCHEM*, 716(1–3), 61–65.
- Şahin, M., Gece, G., Karçı, F., & Bilgiç, S. (2008). Experimental and theoretical study of the effect of some heterocyclic compounds on the corrosion of low carbon steel in 3.5% NaCl medium. *Journal of Applied Electrochemistry*, 38(6), 809–815.
- Sastri, V. S., & Perumareddi, J. R. (1997). Molecular Orbital Theoretical Studies of Some Organic Corrosion Inhibitors. *Corrosion*, 53(8), 617–622.
- Sethuraman, M. G., & Raja, P. B. (2005). Corrosion inhibition of mild steel by Datura metal in acidic medium. *Pigment & Resin Technology*, 34(6), 327–331.
- Umoren, S. A., & Obot, I. B. (2008). Polyvinylpyrrolidone And Polyacrylamide As Corrosion Inhibitors For Mild Steel In Acidic Medium. *Surface Review and Letters*, 15, 277–286.
- Wang, D., Li, S., Ying, Y., Wang, M., Xiao, H., & Chen, Z. (1999). Theoretical and experimental studies of structure and inhibition efficiency of imidazoline derivatives. *Corrosion Science*, 41(10), 1911–1919.
- Wang, H., Wang, X., Wang, H., Wang, L., & Liu, A. (2007). DFT study of new bipyrazole derivatives and their potential activity as corrosion inhibitors. *Molecular Modeling Annual*, 13(1), 147–153.
- Xia, S., Qiu, M., Yu, L., Liu, F., & Zhao, H. (2008). Molecular dynamics and density functional theory study on relationship between structure of imidazoline derivatives and inhibition performance. *Corrosion Science*, 50(7), 2021–2029.
- Yang, W., & Mortier, W. J. (1986). The use of global and local molecular parameters for the analysis of the gas-phase basicity of amines. *J. Am. Chem. Soc.*, 108(19), 5708–5711.
- Zhan, C.-G., Nichols, J. A., & Dixon, D. A. (2003). Ionization Potential, Electron Affinity, Electronegativity, Hardness, and Electron Excitation Energy: Molecular Properties from Density Functional Theory Orbital Energies. *The Journal of Physical Chemistry A*, 107(20), 4184–4195.
- Zhou, G.-d., Feng, Y., Wu, Y., Notoya, T., & Ishikawa, T. (1993). Corrosion Inhibition of Copper by 2-Mercaptobenzothiazole and Benzotriazole in Low-Conductivity Solutions. *Bulletin of the Chemical Society of Japan*, 66(6), 1813–1816.